Dimerosesquiterpene and sesquiterpene lactones from *Artemisia argyi* inhibiting oncogenic PI3K/AKT signaling in melanoma cells

*Lara Dürr,[†] Jakob K. Reinhardt,[†] Maciej Dobrzyński,[‡] Tanja Hell,[†] Martin Smieško,[§] Olivier Pertz,[‡] Matthias Hamburger,[†] Eliane Garo[†,]**

[†] Division of Pharmaceutical Biology, Department of Pharmaceutical Sciences, University of Basel, Klingelbergstrasse 50, 4056 Basel, Switzerland

[‡] Institute of Cell Biology, University of Bern, Baltzerstrasse 4, 3012 Bern, Switzerland

[§] Division of Computational Pharmacy, Department of Pharmaceutical Sciences, University of Basel, Klingelbergstrasse 50, 4056 Basel, Switzerland

*corresponding author: eliane.garo@unibas.ch

ABSTRACT

A library of more than 2'500 plant extracts were screened for their activity on oncogenic signaling in melanoma cells. The ethyl acetate extract from aerial parts of *Artemisia argyi* displayed pronounced inhibition of the PI3K/AKT pathway. Active compounds were tracked with the aid of HPLC-based activity profiling, and a total of 21 active compounds were isolated, including one novel dimerosequiterpenoid (**1**), one new disesquiterpenoid (**2**), three new guaianolides (**3**-**5**), 12 known sesquiterpenoids (**6**-**17**), as well as four known flavonoids (**19**-**22**). A new eudesmanolide derivative (**13b**) was isolated as an artifact formed by methanolysis. Compound **1** is the first adduct comprising a sesquiterpene lactone and a methyl jasmonate moiety. The absolute configurations of compounds **1** and **3**-**18** were established by comparison of experimental and calculated ECD spectra. The absolute configuration for **2** was determined by X-ray diffraction. Guaianolide **8** was the most potent sesquiterpene lactone, inhibiting the PI3K/AKT pathway with an IC_{50} of 8.9 ± 0.9 μM.

Melanoma is the deadliest form of skin cancer, and the incidence rate has been steadily increasing over recent years.[1] Treatment of late-stage metastatic melanoma is challenging because of low patient response to current treatments and rapid development of drug resistance. Uncontrolled cell proliferation in melanoma is driven by activation of the MAPK/ERK (Mitogen-activated Protein Kinase/Extracellular Signal-regulated Kinase) and PI3K/AKT (Phosphatidylinositol 3-kinase/AK strain transforming kinase) pathways (Figure S1, Supporting Information).[2] Various mutations leading to activation of these pathways in melanoma patients are known, including *BRAF*, *NRAS* and *PTEN* mutations. Combination therapies that target the MAPK/ERK signaling pathway at different stages have led to improved progression-free and overall survival.[3] Nevertheless, these treatments only prolong overall survival, and patients relapse after few months. Novel small molecules inhibiting one or both pathways are therefore urgently needed. To identify new inhibitors, a library of 2'500 plant extracts was subjected to a high-content screen (HCS) on two human melanoma cell lines bearing different oncogenic mutations.[4] While the patient-derived cell line MM121224 harbors the classic $BRAF^{T1799A}$ (BRAF V600E) and a $NRAS^{C181A}$ (NRAS Q61K) mutation, the human melanoma cell line A2058 harbors the $BRAF^{T1799A}$ mutation as well as a *PTEN* null mutation (Figure S1, Supporting Information).

The EtOAc extract from aerial parts of *Artemisia argyi* H. Lév. & Vaniot (Asteracae) exhibited promising inhibitory activity on the PI3K/AKT pathway in both melanoma cell lines.[4] HPLC-based activity profiling[5] of the extract and subsequent testing revealed a broad activity window, and on-line spectroscopic data suggested the presence of several structurally similar active compounds in these microfractions. In the course of a metabolomic analysis of several plant extracts, which aimed at establishing a workflow for efficient prioritization of active features in an extract, flavonoids were annotated as being responsible for at least part of the activity of the *A. argyi* extract. These compounds were subsequently isolated to confirm

the annotation.[6] Minor clusters containing sesquiterpene lactones were also highlighted as active (data not shown). Recently, *A. argyi* has been shown to contain a diverse set of sesquiterpene lactones.[7] Moreover, recent clinical studies with the orally-available micheliolide derivative ACT001 suggest that sesquiterpene lactones may be promising candidates for the treatment of advanced solid tumors.[8,9] Therefore, the sesquiterpene lactones present in the active time window of the HPLC-based activity profile were isolated.

Here, we report on the isolation and activity testing of a structurally diverse set of sesquiterpene lactones, including a novel type of dimerosesquiterpene lactone (**1**), a new disesquiterpene lactone (**2**), three new guaianolides (**3**-**5**), along with 17 known compounds.

RESULTS AND DISCUSSION

The DCM and EtOAc library extracts from the aerial parts of *A. argyi* were tested at a concentration of 75 μg/mL in a HCS assay using the MM121224 and A2058 melanoma cell lines.[4] Both extracts strongly inhibited the PI3K/AKT pathway in MM121224 cells, while they mainly displayed toxicity and only weak PI3K/AKT pathway inhibition in A2058 cells. Given that the activity observed in MM121224 cells was promising, both extracts were submitted to HPLC-based activity profiling.[5] The activity profiles of both library extracts showed distinct and localized activity on AKT in MM121224 cells (Figures S3 and S4, Supporting Information).

A scale-up EtOAc extract of *A. argyi* (AE-SU) was analyzed by HPLC-based activity profiling (Figure 1). Given that the profile was similar to the DCM library extract, AE-SU was subsequently used for isolation of the active compounds.

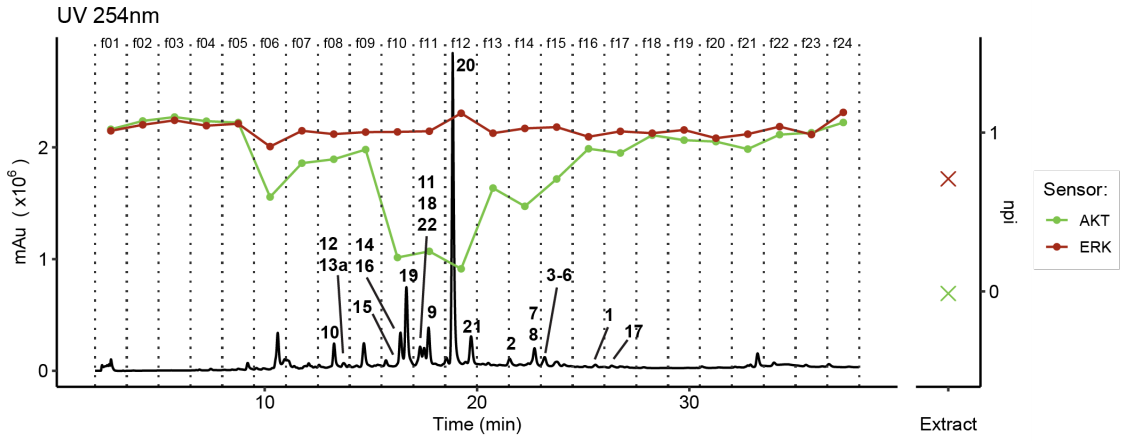

Figure 1. HPLC-based activity profile of the *Artemisia argyi* EtOAc (AE-SU) extract. The normalized percentage of AKT (green) and ERK (red) inhibition in MM121224 cells is shown above the HPLC chromatogram recorded at 254 nm. The activity of the extract is displayed on the right of the chromatogram. Dotted lines indicate the microfractions collected for the bioassay. Bold numbers refer to compounds **1-22**. The chromatogram is shown from min 2 to 38.

Chart 1

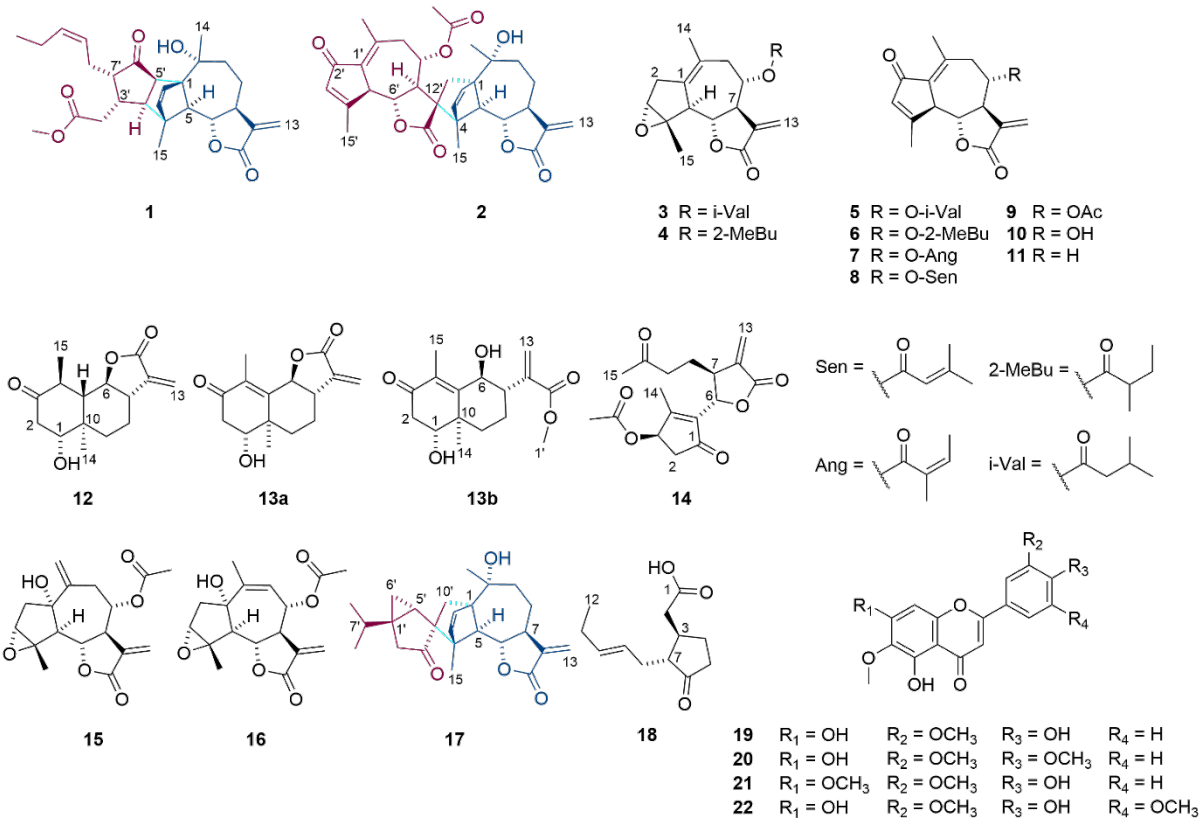

Compound **1** had a molecular formula of $C_{28}H_{36}O_6$, as established by HRESIMS (*m/z* 469.2572 $[M + H]^+$, calcd. for $C_{28}H_{37}O_6$, 469.2585), and NMR data (Table 1), indicating 11 degrees of unsaturation. The NMR data further revealed the presence of 9 sp^2 carbons (3 carbonyl and 6 olefinic carbons) suggesting a pentacyclic scaffold. The COSY and HMBC spectra indicated the presence of two distincts parts in the molecule. The presence of two olefinic protons (δ_H 5.91, δ_H 6.03), two exocyclic methylene protons (δ_H 5.89/5.43), three methine (δ_H 4.01, δ_H 3.11, δ_H 1.88), two methylene (δ_H 1.29/2.13, δ_H 1.61/1.66) and two methyl groups (δ_H 1.39, δ_H 1.33) were indicative of a guaianolide sesquiterpene lactone. The spin system from H-5 to H-9b in the COSY spectrum, and key HMBC correlations from H_3-14 to C-1 and C-9, from H-5 to C-10, and from H_3-15 to C-5 completed the assignment of the guaianolide sesquiterpene lactone motif in **1**.

The second part of the molecule was characterized by a carboxyl group at δ_C 216.9 (C-6') and four methine protons at δ_H 2.26, 2.23, 3.28 and 2.27 (C-3', C-4', C-5', C-7') indicating a cyclopentanone ring. Additional signals for two olefinic protons (δ_H 5.34, δ_H 5.23), two methylene (δ_H 1.77/2.15, δ_H 1.96) and one methyl (δ_H 0.89) group were assigned to a 2-pentene aliphatic chain attached at C-7'. The assignments were corroborated by COSY and HMBC data. Finally, the remaining signals for one carbonyl (δ_C 172.5), one methylene (δ_H 2.07/2.34) and one methoxy (δ_H 3.59) group were all assigned to an ethanoic acid methyl ester residue attached at C-3' (HMBC correlations from H_2-2' to C-1', C-3', C-4', and C-7', as well as from CH_3-13' to C-1'). Overall, carbons C-1' to C-13' originated from a methyl jasmonate moiety, and HMBC correlations of H-4' to C-3 and C-15, and from H-5' to C-2 and C-10 established the attachment of this residue at C-1 and C-4 of the guaianolide moiety (Figure 2A).

The relative configuration of the seven-membered ring was established through NOESY correlations of H-5/H-7 and H-6/H-8b, and defined H-5 and H-7 as α-oriented. Thus, NOESY crosspeaks between H-6/H-2 and H_3-14/H-2 indicated that H_3-14 and the bridging cyclopentene ring were in β-orientation (Figure 2B). Moreover, NOESY correlations between H-3'/H-3 and H-7'/H-2 indicated a *cis*-β-orientation of H-3' and H-7'. This assignment was supported by crosspeaks between H-2'b/H_2-8' and H_3-15/H-3'. The α-orientation of H-4' and H-5' was indicated by crosspeaks of both protons with H-5.

The absolute configuration was assigned by comparison of experimental and calculated ECD spectra. The experimental spectrum of **1** showed positive CEs at 199 and 304 nm, and a negative CE at 221 nm (Figure 2C). Thus, the absolute configuration of compound **1** was assigned as 1*R*,4*S*,5*S*,6*S*,7*S*,10*R*,3'*S*,4'*S*,5'*R*,7'*S*. In conclusion, artejasminolide (**1**) is a novel natural product combining a guaianolide sesquiterpene lactone (part A) with methyl *cis*-jasmonate (part B). This is the first case of a dimerosesquiterpenoid lactone containing a jasmonate moiety.

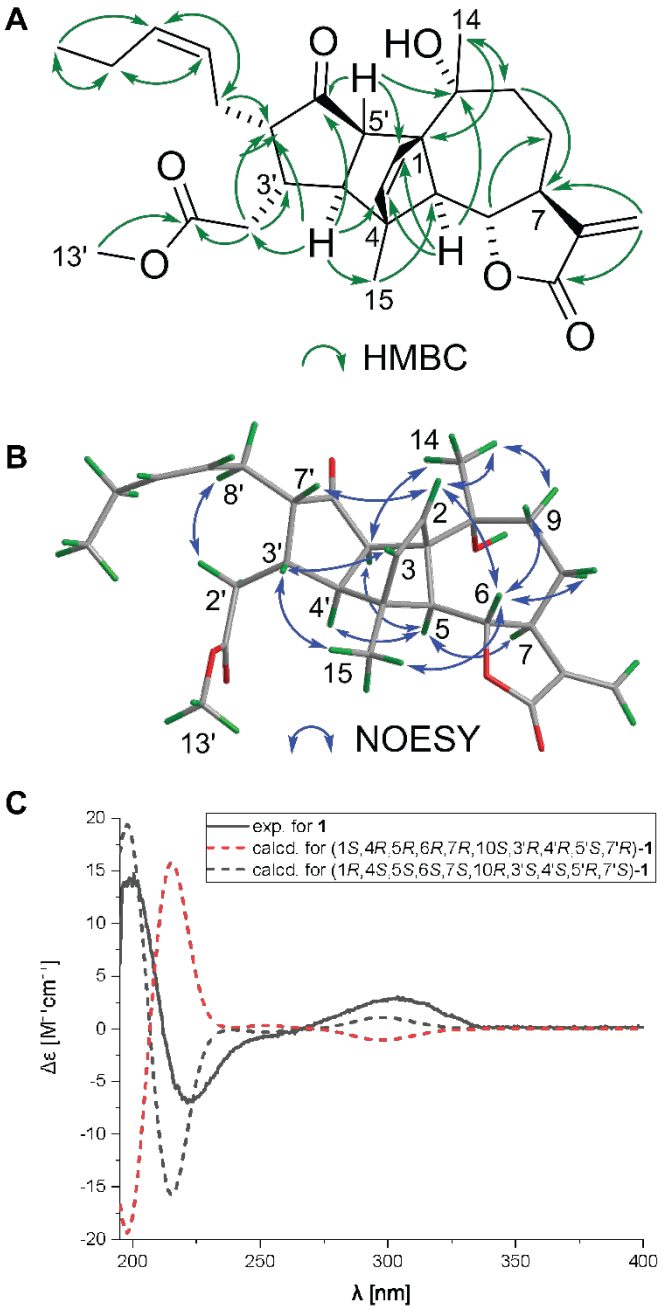

Figure 2. (A) Key HMBC correlations, (B) Key ROESY correlations, and (C) Experimental and calculated ECD spectra of **1**.

Table 1. ^{1}H (500 MHz) and ^{13}C (125 MHz) NMR Spectroscopic Data of Compounds 1 and 2

	1		**2**	
no.	**δ_C, type**	**δ_H, mult. (*J* in Hz)**	**δ_C, type**	**δ_H, mult. (*J* in Hz)**

1	71.9, C		63.3, C	
2	134.6, CH	5.91, d (5.8)	133.2, CH	5.85, d (5.7)
3	136.8, CH	6.03, d (5.8)	141.2, CH	6.16, m[a]
4	54.7, C		56.2, C	
5	72.6, CH	1.88, d (9.8)	66.1, CH	1.85, d (9.8)
6	78.7, CH	4.01, dd (9.8, 9.8)	79.5, CH	4.10, dd (9.8, 9.8)
7	42.7, CH	3.11, ddddd (9.9, 9.8, 8.1, 3.7, 3.4)	43.0, CH	3.02, m[a]
8a	23.5, CH_2	1.29, m[a]	23.6, CH_2	1.33, m
8b		2.13, m[a]		2.14, m
9a	35.8, CH_2	1.61, m[a]	34.3, CH_2	1.68, m
9b		1.66, m[a]		
10	72.2, C		71.0, C	
11	169.8, C		170.0, C	
12	141.4, C		140.9, C	
13a	118.3, CH_2	5.43, d (3.5)	119.2, CH_2	5.46, d (3.4)
13b		5.89, d (3.5)		5.94, d (3.7)
14	30.3, CH_3	1.39, s	28.9, CH_3	1.15, s
15	16.9, CH_3	1.33, s	14.5, CH_3	1.43, s
1'	172.5, C		134.3, C	
2'a	36.0, CH_2	2.07, dd (15.3, 8.2)	194.5, C	
2'b		2.34, dd (15.3, 3.1)		
3'	31.8, CH	2.26, m[a]	135.4, CH	6.18, m[a]
4'	53.9, CH	2.23, d 8.7)	171.8, C	
5'	54.4, CH	3.28, d (8.7)	48.9, CH	3.84, d (10.2)
6'	216.9, C		79.0, CH	3.75, d (10.2, 10.2)

7'	53.7, CH	2.27, m[a]	55.2, CH	3.03, m[a]
8'a	22.8, CH_2	1.77, ddd (15.6, 8.1, 8.1)	66.3, CH	4.95, ddd (10.5, 10.5, 2.0)
8'b		2.15, m[a]		
9'a	126.9, CH	5.23, m	42.4, CH_2	2.23, m[a]
9'b				2.91, dd (12.8, 10.5)
10'	132.2, CH	5.34, m	142.8, C	
11'	20.2, CH_2	1.96, qd (7.4, 7.4)	176.2, C	
12'	14.0, CH_3	0.89, t (7.5)	59.4, C	
13'a	51.4, CH_3	3.59, s	36.3, CH_2	1.39, d (12.3)
13'b				2.41, d (12.3)
14'			19.4, CH_3	2.28, s
15'			19.9, CH_3	2.22, s
1''			169.2, C	
2''			21.4, CH_3	1.90, s

[a] Overlapping signals.

Compound **2** had a molecular formula of $C_{32}H_{36}O_8$, as established by HRESIMS (*m/z* 549.2470 $[M + H]^+$, calcd for $C_{32}H_{37}O_8$, 549.2483) and NMR data (Table 1), indicating 15 degrees of unsaturation. Analysis of the NMR data suggested that **2** consisted of two parts, both containing a γ-lactone ring. Part A was found to be identical to the guaianolide substructure in **1**. The remaining ^{1}H-NMR signals for one olefinic proton (δ_H 6.18), four methines (δ_H 3.84, δ_H 3.75, δ_H 3.03, and δ_H 4.95), two methylene (δ_H 2.23/2.91, δ_H 2.41/1.39), two methyl groups (δ_H 2.28, δ_H 2.22) and one acetyl group (δ_C 169.2; δ_C 21.4, δ_H 1.90) implied a second guaianolide scaffold (part B). The position of the acetyl group at C-8' was assigned from the contiguous spin system between H-5' and H-9' observed in the COSY spectrum, and

by an HMBC correlation from H-8' to C-1'' (Figure 3A). The orientation of the cyclopentanone ring was established by diagnostic HMBC correlations from H_3-15' to C-2', C-3', C-4', C-5', and C-6'. The γ-lactone ring was characterized through HMBC correlations from H-6' to C-12', and from H-7' to C-11' and C-13'. Finally, the linkage of the two sesquiterpene substructures A and B were determined through key HMBC cross-peaks from H_2-13'b to C-1, C-2, C-10, and from H_3-15 to C-12'.

The relative configuration of **2** was established by a ROESY spectrum (Figure 3C). The relative configuration of part A was found to be identical to **1**. The relative configuration of part B was determined by correlations between H-5'/H-7', and H-6'/H-8', respectively. The configuration at C-12' was established by ROESY crosspeaks between H_3-15/H-7', and between H-6'/H-8' and H-6'/H_2-13' (Figure 3C). The absolute configuration was determined by single crystal X-ray diffraction (Figure 3B) providing the absolute configuration as 1*R*,4*R*,5*S*,6*S*,7*S*,10*R*,5'*S*,6'*R*,7'*R*,8'*S*,12'*R*. This was confirmed by comparing the experimental ECD spectrum of **2** to *ab initio* calculated spectra (Figure 3D). Compound **2** was named 8-acetyl *epi*-arteminolide. It is noteworthy that C-12'*S*-epimer of **2**, 8-acetyl arteminolide, was recently reported from the same extract.[7]

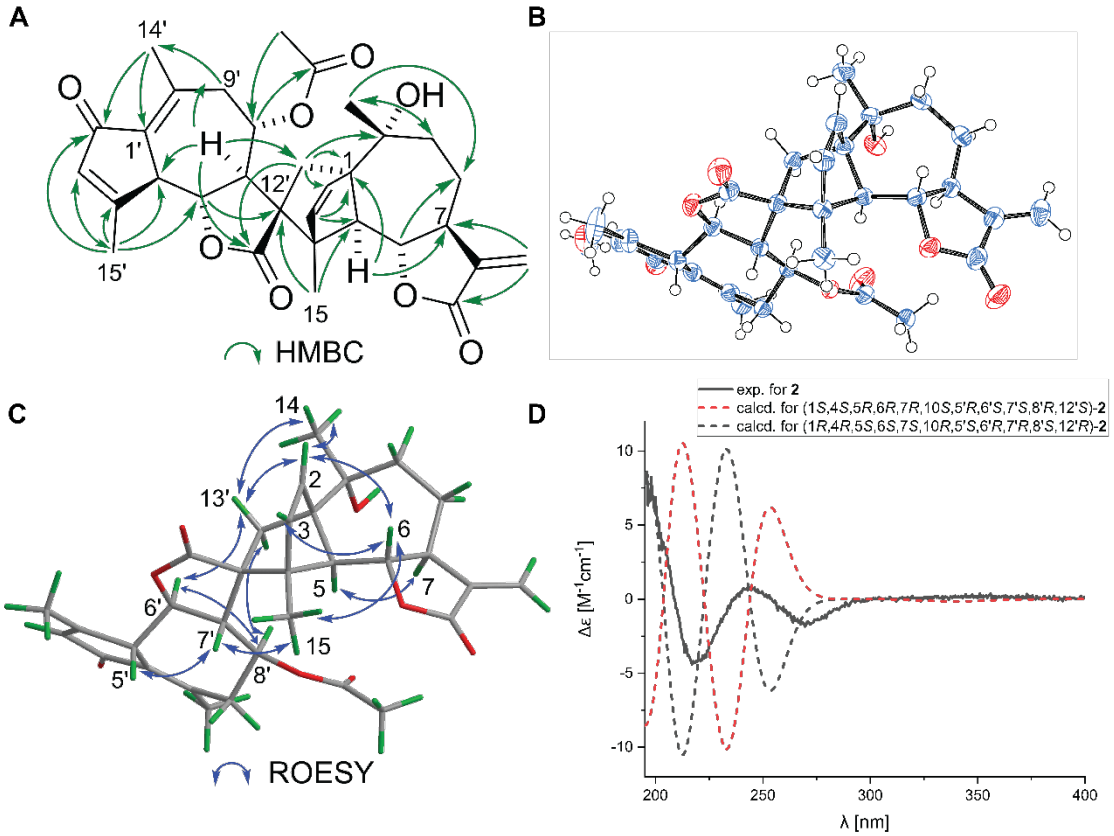

Figure 3. (A) Key HMBC correlations, (B) Key ROESY correlations, (C) ORTEP drawing of the structure obtained from single crystal X-ray diffraction (ellipsoids at 50% probability), and (D) Experimental and calculated ECD spectra of **2**.

Compound **3** was analyzed by HRESIMS (347.1843 $[M + H]^+$, calcd for $C_{20}H_{27}O_5$, 347.1853) and NMR as $C_{20}H_{26}O_5$, a molecular formula requiring eight degrees of unsaturation. In the NMR data, signals for one carbonyl (δ_C 168.5), one exomethylene, five methine and two methyl groups were characteristic of a guaianolide sesquiterpene. HMBC correlations indicated the presence of an epoxy group at C-3 and C-4, a double bond between C-10 and C-1, and a substituent at C-8. One methine (δ_H 2.27), one methylene (δ_H 2.02), and two equivalent methyl groups (δ_H 0.93) in the ^{1}H-NMR spectrum indicated an isovaleroyl moiety that was attached at C-8 (HMBC correlation from H-8 to C-1').

The relative configuration was established by NOESY data. Assuming an α-orientation for H-5, the correlations between H-5/H-7 and H-6/H-8 indicated that H-7 was α-oriented, while

H-6 and H-8 were both β-oriented (Figure 4A). The relative configuration at C-4 was more challenging, given that NOESY correlations between H_3-14/H-6 and H_3-14/H-5 were compatible with both possible orientations of the epoxy group. Solely the NOESY crosspeak between H-6/H-2a hinted the epoxy group to be α-oriented. Analyzing the C-5 chemical shifts in similar compounds found C-5 to be more shielded with β-oriented epoxy-groups (δ_C 42.5, **26**[7]) than with α-oriented groups (δ_C 50.3 for **23**[7] and δ_C 51.2 for **35**[7]). Thus, the chemical shift observed for C-5 (δ_C 50.3) in **3** corroborated the assignment via NOESY and showed the epoxy group to be α-oriented.

The absolute configuration was established by ECD. The experimental spectrum displayed a positive CE at 210 nm and a negative CE at 230 nm and was in agreement with the calculated spectrum of the 3*R*,4*S*,5*S*,6*S*,7*R*,8*S* stereoisomer. This new compound **3** was named argyinolide O.

The ^{1}H NMR spectrum of **4** was similar to that of **3**. The only difference was in the presence of two methyl groups of the side chain that were appearing as triplet and doublet, respectively, instead of two singlets. The data were in accord with a 2-methyl-butanoyl moiety attached to C-8. The relative and absolute configuration of **4** was determined with the aid of NOESY (Figure 4B) and ECD spectra as 3*R*,4*S*,5*S*,6*S*,7*R*,8*S*. The configuration at C-2' could not be established due to the lack of a chromophore in the side chain. A stereoisomer of **4** bearing a β-orientated epoxide was reported recently.[10] Given that the NMR data for that compound were virtually identical to those of **4**, its proposed structure is likely incorrect. Sesquiterpene lactone **4** is a new natural product that was named argyinolide P.

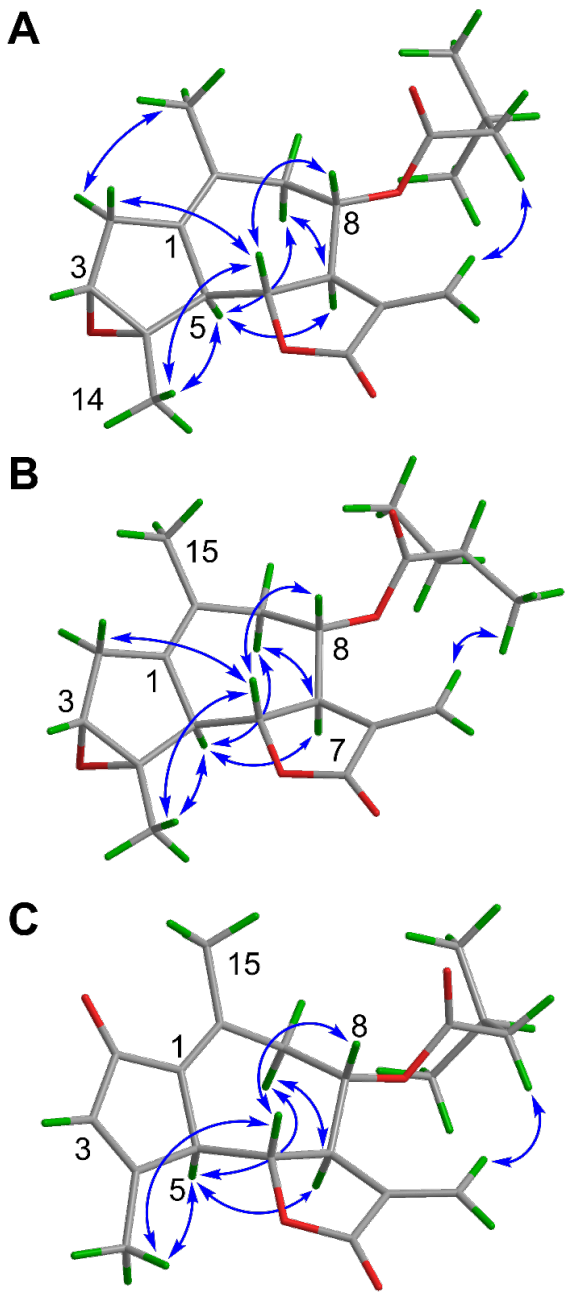

Figure 4. Key NOESY correlations (blue arrows) of compounds **3** (A), **4** (B) and **5** (C).

Table 2. ^{1}H (500 MHz) and ^{13}C (125 MHz) NMR Spectroscopic Data of Compounds 3, 4 and 5

	3		**4**		**5**	
no.	**δ_C, type**	**δ_H, mult. (*J* in Hz)**	**δ_C, type**	**δ_H, mult. (*J* in Hz)**	**δ_C, type**	**δ_H, mult. (*J* in Hz)**
1	136.8, C		136.9, C		133.5, C	

2a	32.9, CH_2	2.46, m[a]	32.9, CH_2	2.46, m[a]	194.7, C	
2b		2.55, m[a]		2.54, m[a]		
3	62.7, CH	3.43, m[a]	62.7, CH	3.43, m[a]	135.1, CH	6.21, s
4	65.9, C		65.9, C		170.4, C	
5	50.2, CH	3.18, br d (11.3)	50.1, CH	3.19, d (10.7)	50.1, CH	3.83, d (10.1)
6	77.4, CH	3.95, dd (10.2, 10.2)	77.4, CH	3.96, dd (10.4, 10.4)	80.9, CH	3.97, dd (10.1, 9.9)
7	54.5, CH	3.40, m[a]	54.5, CH	3.42, m[a]	53.0, CH	3.58, br dd (10.1, 9.9)
8	69.9, CH	4.70, ddd (10.5, 10.5, 2.0)	69.9, CH	4.71, ddd (10.5, 10.5, 1.9)	68.9, CH	4.88, dd (10.1, 10.1)
9a	40.6, CH_2	2.01, m[a]	40.4, CH_2	1.97, dd (13.3, 1.9)	43.4, CH_2	2.27, m[a]
9b		2.52, m[a]		2.53, m[a]		2.86, dd (12.3, 10.1)
10	126.7, C		126.6, C		144.0, C	
11	168.5, C		137.5, C		136.6, C	
12	137.3, C		168.4, C		168.4, C	
13a	119.7, CH_2	5.51, d (2.7)	119.4, CH_2	5.48, d (2.7)	120.8, CH_2	5.61, d (2.4)
13b		5.99, d (3.4)		5.99, d (3.0)		6.04, d (2.4)
14	21.8, CH_3	1.64, s	21.7, CH_3	1.64, s[a]	20.7, CH_3	2.33, s[a]
15	18.9, CH_3	1.51, s	18.9, CH_3	1.52, s	19.5, CH_3	2.24, s[a]
1'	171.6, C		174.9, C		171.6, C	
2'	42.5, CH_2	2.27, dd (7.2, 2.6)	40.5, CH	2.41, m[a]	42.4, CH_2	2.31, m[a]
3'a	25.1, CH	2.02, m[a]	25.9, CH_2	1.43, m	25.1, CH	2.03, m
3'b				1.63, m[a]		
4'	22.1, CH_3	0.93, d (6.7)	11.5, CH_3	0.88, t (7.5)	22.1, CH_3	0.94, d (6.7)

5'	22.1, CH_3	0.93, (6.7)	d	16.5, CH_3	1.11, d (7.0)	22.1, CH_3	0.94, d (6.7)

[a] Overlapping signals.

Compound **5** had a molecular formula of $C_{20}H_{24}O_5$, as established by HRESIMS (*m/z* 345.1697 $[M + H]^+$, calcd for $C_{20}H_{25}O_5$, 345.1697) and NMR data (Table 2) indicating nine degrees of unsaturation. NMR analysis showed that **5** shared the same scaffold as artemdubolide C (**6**), the only difference being in the substituent at C-8. The ^1H NMR spectrum showed signals for one methine (δ_H 2.03), one methylene group (δ_H 2.31) and two equivalent methyl groups (δ_H 0.94) characeteristic of an isovaleryl moiety. The relative configuration of the α-methylene-γ-unsaturated lactone moiety was deduced from NOESY correlations between H-5/H-7 and H-5/H-9b, and between H-6/H-8 (Figure 4C). The absolute configuration of **5** was determined by ECD (Figure S68, Supporting Information). The experimental spectrum of **5** displayed a positive CE at 246 nm, and negative CEs at 226 and 270 nm. Comparison with the calculated spectra for both enantiomers enabled compound **5** to be assigned as 5*S*,6*R*,7*R*,8*S*. Compound **5** is a new natural product and was named argyinolide Q.

The NMR analysis of compounds **6**-**11** indicated that they differed from **5** by the acyl residues at C-8. They were identified as artemdubolide C (**6**),[11] moxartenolide (**7**),[12] artemisiane E (**8**),[13] 11,13-dehydromatricarin (**9**),[14,15] 11,13-dehydrodesacetylmatricarin (**10**),[16,17] and dehydroleucodine (**11**)[18].

The experimental ECD spectra for **6**-**11** were all similar to that of **5**, and the absolute configurations of **8**, **10** and **11** (Figures S71, 73, 74, Supporting Information) were in accordance with literature. The absolute configurations of **6**, **7** and **9** had not been previously reported and were determined as 5*S*,6*R*,7*R*,8*S* (Figures S69, S70, S72, Supporting Information). The absolute configuration at C-2' in artemdubolide C (**6**) was not assigned.

Compounds **12** and **13a** were identified as the eudesmanolides artecalin[19,20] and armexifolin[21]. When **13a** was kept in MeOH for 24h at RT, HPLC-MS analysis unexpectedly revealed two peaks. The first peak (*m/z* 263 $[M+H]^+$) corresponded to **13a**, while the second peak (*m/z* 295 $[M+H]^+$) indicated addition of MeOH. After standing for 5 days in MeOH at RT, sufficient degradation product was formed for HRMS and NMR analysis, and **13b** was identified as methyl ester **13b** formed by methanolysis of the lactone ring (Figure S83, Supporting Information).

ECD spectra were measured for **12, 13a**, and **13b**. The data of **12** were in good agreement with literature,[19,22] while the absolute configuration of **13a** had not been reported. The experimental spectra of **13a** and **13b** displayed a positive CE at 250 nm, and a negative CE at 315 nm. Comparison with calculated spectra established the absolute configuration of both compounds as 1*R*,6*S*,7*S*,10*R* (Figures S76 and S77, Supporting Information).

Sesquiterpene lactone **14** was identified as 3-O-acetyl-iso-*seco*-tanapartholide.[23] With the aid of experimental and calculated ECD spectra the absolute configuration was determined as 3*R*,6*S*,7*S* (Figure S78, Supporting Information).

Compounds **15** and **16** showed highly similar NMR data, and slight differences were observed only for C-9, C-10 and C-15. Compound **15** was identified as arteglasin B.[24] The known compound **16** [25] was named argyinolide R. As the absolute configurations of both compounds have not been reported, they were determined by ECD. The experimental ECD spectra for both compounds showed strong positive CEs at 200 nm. A comparison of the experimental and calculated ECD spectra for **15** suggested the absolute configuration as 1*S*,3*R*,4*S*,5*R*,6*S*,7*R*,8*S* (Figure S79, Supporting Information). The calculated ECD spectrum of compound **16** (Figure S80, Supporting Information), suggested the opposite enantiomer for **16**, which, however, seemed highly unlikely.

A re-examination of the NOESY spectra of **15** and **16** showed unusual crosspeaks between H-2a (δ_H 2.49)/H-5 (δ_H 2.58) and a broad water signal at δ_H 1.59. The water signal in both spectra integrated for two protons, thereby indicating a single water molecule coordinated via hydrogen bonds with OH-1 and the epoxy-O. To verify whether a water molecule would assume this position, a conformational search of both compounds in the presence of a single water molecule was performed. A total of 20 conformers were calculated for each compound. Of these, one conformer of **15** (conformer 1, Figure 5A) and two conformers of **16** (conformers 7 and 17, Figure 5B) had the water molecule in the expected position.

Thus, ECD spectra were calculated and Boltzmann-averaged for i) conformers calculated without water (calcd. for 1*S*,3*R*,4*S*,5*R*,6*S*,7*R*,8*S*), ii) all conformers with one water molecule regardless of its position (calcd. for 1*S*,3*R*,4*S*,5*R*,6*S*,7*R*,8*S* + H_2O) and, iii) conformers with the water molecule coordinated as predicted by the NMR data (1*S*,3*R*,4*S*,5*R*,6*S*,7*R*,8*S* + >O···H_2O···HO-) (Figure 5). Interestingly, only iii) led to significant changes in the calculated ECD spectra. In case of **15**, a positive CE at 200 nm was predicted in all three calculated spectra, consistently leading to an assignment of its absolute configuration as 1*S*,3*R*,4*S*,5*R*,6*S*,7*R*,8*S*. For **16**, however, only iii) with the coordinated water molecule resulted in a strong positive CE at 200 nm, indicating the absolute configuration to be consistent with **15**. Although this is far from being a quantitative approach, the case of **16** highlights possible effects of coordinated water molecules on the ECD spectra and, as a consequence, on the assignment of the absolute configuration. Thus, the absolute configuration of **16** was assigned as 1*S*,3*R*,4*S*,5*R*,6*S*,7*R*,8*S*.

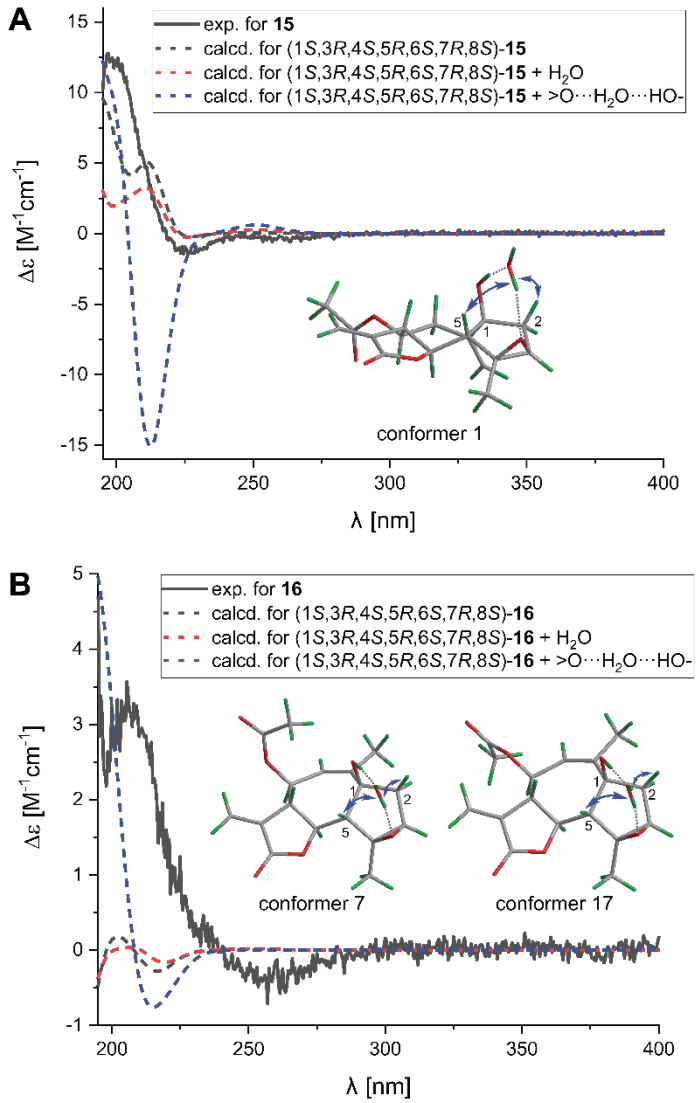

Figure 5. ECD experimental spectra (black) of **15** (A) and **16** (B), and calculated spectra for three stereoisomers, together with the three major conformers that were in accord with the NOESY data (correlations shown as blue arrows). Three ECD spectra were computed for **15** and **16**, namely the spectrum from conformers obtained without water (hashed black line, 11 and 7 conformers, respectively), the spectrum from conformers obtained with a water molecule coordinated anywhere in the structure (hashed red line, 20 conformers each), and the spectrum containing only the conformers obtained with a water molecule, where the water molecule was coordinated between the OH-1 and the oxygen of the epoxide moiety (hashed blue line, depicted conformers).

Compound **17** and **18** were identified as artemisolide and (-)-jasmonic acid respectively.[26,27] The NMR data and absolute configurations found through ECD analysis (Figures S81 and S82, Supporting Information) were in agreement with published data. The UV spectra of compounds **19-22** (absorption maxima between 270 and 275 nm, and 340-345 nm) were indicative of flavones. Jaceosidin (**19**), eupatilin (**20**), chrysosplenitin (**21**) and 6-methoxytricin (**22**) have all been previously reported from *Artemisia* species.[7,28–30]

Sesquiterpene lactones containing a cyclopentadiene can undergo Diels-Alder-like [4+2]-cycloaddition reactions with dienophiles.[31] Disesquiterpenoid lactones, such as **2** are formed by a cycloaddition reaction with other sesquiterpene lactones, while dienophiles of other biosynthetic origins (methyl jasmonate, monoterpene) lead to dimerosesquiterpenoid lactones, such as **1** and **17**. Compound **2** highlights the diversity of possible disesquiterpenoids. Depending on the relative position of the two sesquiterpene parts during the reaction, the cycloaddition can lead to different isomers. Disesquiterpenoid **2**, along with other known analogues reported in the literature, exemplify four different ways by which both parts can be linked together.[7,15,32] As shown in Scheme S1, the cycloaddition can happen by the addition of the dienophile B to the front or the back of the cyclopentadiene moiety of the guaianolide A. This leads to different orientations of the C-2/C-3 bridge and, therefore, to different configurations at C-4. In addition, the relative orientation of part B determines the configuration at C-12'. Thus, a total of four isomers are possible outcomes, and the naming of these isomers has been based on the configurations at C-4 and C-12'. The suffix "-minolide" has been given to dimers with a 4*R*-configuration[33], and "-maloide" for the 4*S*-configuration.[34] For dimers with a 12'*R*-configuration the prefix *epi*- is added to the name. Thus, compound **2** was named 8-acetyl *epi*-arteminolide. From the four possible combinations shown in Scheme S1, the (12'*R*, 4*S*) isomer (*epi*-*-maloide) has not been isolated so far.

Another notable finding was the (3'*S*,7'*R*)-*cis*-configuration of the methyl jasmonate-derived moiety in **1,** while the related (-)-jasmonic acid (**18**) was the (3*R*,7*R*)-*trans*-stereoisomer. Biosynthetically, jasmonates are produced as *cis*-jasmonic acid, followed by spontaneous epimerization into the more stable *trans*-jasmonic acid.[35,36] Thus, the *cis*-methyl jasmonate moiety in **1** underscores the natural origin of **1**, as opposed to it being a possible artefact of isolation or storage. A possible biological role of **1** in the context of the jasmonate class of plant hormones remains to be investigated.

PI3K/AKT pathway inhibition. Compounds **1**-**22** were tested in MM121224 and A2058 melanoma cells. In addition, the compounds **23**-**37** previously isolated from *A. argyi* were also tested (Figure S84 and S85, Supporting Information).[7] In MM121224 cells all compounds, with the exception of jasmonic acid (**18**), showed an effect on the AKT-KTR to varying degrees, but none of the compounds affected the ERK-KTR. Compounds with IC_{50} values < 20 μM were considered as active. A2058 cells were more sensitive to the toxicity of the sesquiterpene lactones, and only marginal activity on the PI3K/AKT pathway was seen (data not shown). Therefore, only the results obtained with the MM121224 cell line are discussed (Figures S87-95, Supporting Information).

The most active sesquiterpene lactones were guaianolides **7**-**9**, and the eudesmanolide **13a** (IC_{50} < 12 μM) as shown in Table 1. The concentration-dependent response of the most promising compound (**8**) (IC_{50} 8.9 ± 0.9 μM; Figure 6) revealed strong inhibition at 25 μM, and toxicity at the highest concentrations (200 to 50 μM; data not shown). Additional images are provided for selected compounds (**7**, **8**, **9**, **13a**; Figures S96-99, Supporting Information).

The sesquiterpene lactones displayed toxicity at higher concentrations. As a 100% inhibition of AKT activity was not always measurable, sigmoidal curve fitting for calculation of the relative IC_{50} values was not possible for these compounds. In such cases, the absolute IC_{50} (the

concentration that leads to 50% inhibition relative to the positive control) were calculated (Table 1). For **4**, **12**, **27**, **29/30** and **36** no IC_{50} values could be obtained.

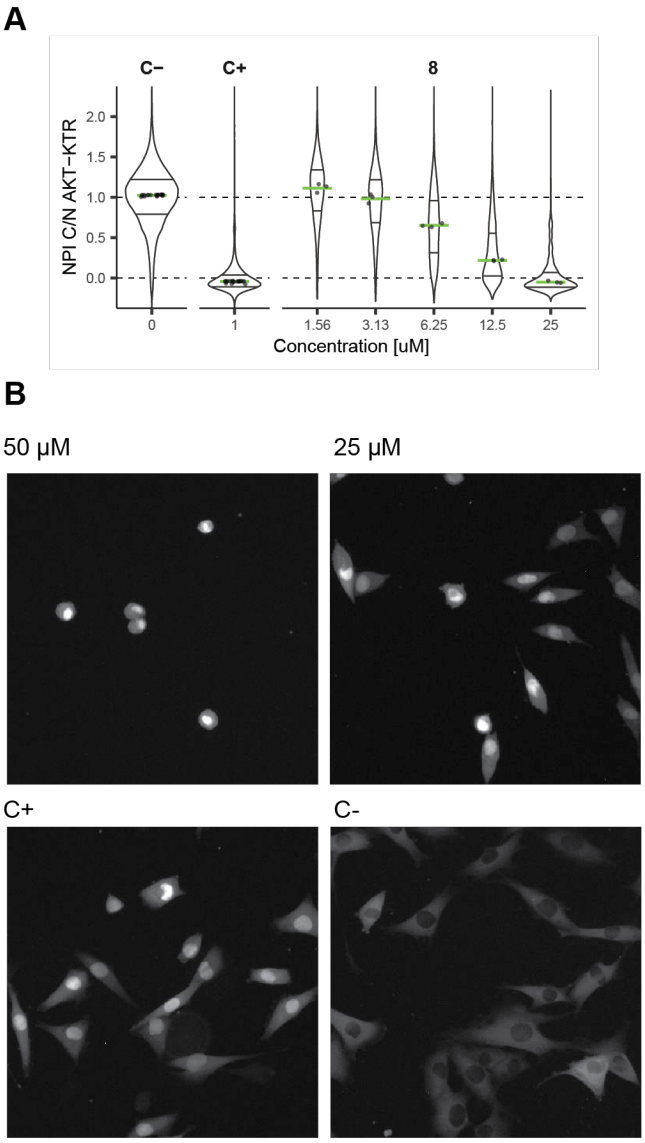

Figure 6. Effect of **8** on ATK activity in MM121224 cells. (A) Concentration response, where data distribution from single cells are represented as violin plots. Median of treatment distribution (middle bar, green), as well as first and third quartiles are shown. Data were taken from at least 200 cells. (B) Representative images of MM121224 cells treated with 50 and 25 μM of **8**. The image shows 11.5% of the full field of view. The brightness was adapted same for all images. C+ and C- designate positive (1 μM GDC0941 as PI3K/AKT pathway inhibitor) and negative (0.75% DMSO) controls, respectively.

Table 1. Activities of Selected Compounds on the PI3K/AKT pathway in MM121224 Cells

compound[a]	IC_{50} values [μM]
1	27.7 ± 1.2
2	35.7 ± 4.9
3	16.9 ± 3.8[b]
5	15.3 ± 2.0[b]
6	27.7 ± 2.4
7	9.8 ± 0.7
8	8.9 ± 0.9
9	11.0 ± 0.6[b]
10	15.1 ± 1.0[b]
11	23.6 ± 4.9
13a	11.2 ± 1.5[b]
13b	22.1 ± 4.4[b]
14	25.1 ± 2.0
15	46.2 ± 15.3[b]
16	22.9 ± 4.5
17	26.5 ± 1.2
23	119.1 ± 31.2[b]
24	22.5 ± 0.9
25	38.0 ± 1.5
26	38.4 ± 5.8[b]
28	52.7 ± 3.4
31	24.6 ± 1.1
32	27.9 ± 1.1
33/34	14.2 ± 1.3
35	25.9 ± 4.9[b]
37	14.7 ± 1.2

[a] Compounds **4**, **12**, **27**, **29/30** and **36** could not be fitted for a calculation of relative or absolute IC_{50} values

[b]absolute IC_{50} value

For selected sesquiterpene lactones (**1**, **2**, **10**, **13a**, **13b**, **14**) the inhibition of AKT activity was confirmed with immunostaining experiments (Figures S100 and S101, Supporting Information).

Sesquiterpene lactones have been associated with cytotoxicity and potential anticancer activity.[37] The cytotoxic properties have been investigated and explained, at least in part, by the electrophilic properties of α,β-unsaturated carbonyl groups and/or α-methylene-γ-lactone moieties. Via a Michael addition they can form covalent bonds with thiol groups in proteins and, thereby, block protein activity.[38–41] This unspecific mechanism of action can also affect essential enzymes, thereby leading to general cytotoxicity. However, ACT001, a derivative of the guaianolide micheliolide, successfully completed phase I clinical trials for the treatment of advanced solid tumors, including glioblastoma. The compound showed preliminary evidence of antitumor activity, satisfactory bioavailability and good tolerability. This example highlights the potential of sesquiterpene lactones in cancer therapy.[8,42]

The flavonoids were the most active compounds without displaying toxicity. As recently reported, the most active flavonoid on the PI3K/AKT pathway in MM121224 cells was **22** (IC_{50} of 4.9 ± 0.2 μM).[6] In A2058 cells, compound **22** was also the most active flavonoid (IC_{50} of 26 ± 1.8 μM; Figure S86, Supporting Information). The difference in activity in the two cell lines might be due to their mutational landscape. In A2058 cells the pathway is activated by a loss of PTEN lipid phosphatase, while in MM121224 the oncogenic signaling is due to crossactivation by NRAS (Figure S1, Supporting Information). Therefore, it is likely more difficult to inhibit aberrant signaling caused by the absence of a protein.[4]

Future investigations will clarify whether the inhibitory properties of the sesquiterpenes was due to their alkylating properties, or to other modes of action. Target identification for the most potent sesquiterpene lactones (**7**-**9**, **13a**) will be achieved with cellular thermal shift assays [43] or thermal proteome profiling.[44]

EXPERIMENTAL SECTION

General Experimental Procedures. Optical rotations were measured in MeOH or $CHCl_3$ on a JASCO P-2000 polarimeter (Brechbühler) equipped with a 10 cm temperature-controlled microcell. ECD and UV spectra were recorded in MeOH (83.25 – 333.3 μg/mL) on a Chirascan CD spectrometer using 1 mm path precision cells (110 QS, Hellma Analytics). NMR spectra were recorded on a Bruker Avance III NMR spectrometer operating at 500.13 MHz for ^{1}H and 125.77 MHz for ^{13}C, equipped with a 1 mm TXI microprobe or a 5 mm BBO probe, operated at 23 °C. Spectra were recorded at 23 °C in $CDCl_3$ (Sigma-Aldrich/Merck) or DMSO-*d6* (both Armar Chemicals) and analyzed by Bruker TopSpin 3.5 and ACD/Labs NMR Workbook suite software. Chemical shifts are reported as δ values (ppm), with residual signal as internal reference, *J* in Hz.

HPLC-grade solvents (Macron/Reuss Chemie/Scharlau) and ultrapure water from a Milli-Q water purification system (Merck Millipore) were used for analytical and semi-preparative HPLC separations. DMSO, HPLC-grade formic acid (FA), and solvents were obtained from Macron Fine Chemicals or Scharlau. For the purpose of extraction and preparative separation, technical-grade solvents were used after distillation. Normal-phase flash chromatography was carried out on a Puriflash 4100 system (Interchim) consisting of a pump, UV detector and fraction collector. Silica gel 60 (15 - 40 μm to pack column; 63 - 200 μm for dry loading of sample) was from Merck. Column dimensions 45 × 3.5 cm. Flow rate was 20 mL/min. Preparative HPLC separation was performed on a 1290 Infinity II Preparative LC system

(Agilent Technologies) consisting of a binary pump (1260 Prep Bin Pump) connected to a PDA (1100 Series). Data acquisition and processing were carried out with Chemstation (Agilent Technologies). A SunFire Prep C_{18} OBD column (5 μm, 150 × 30 mm i.d., Waters) equipped with a C_{18} Prep guard column (10 × 30 mm i.d.) was used with a flow rate of 20 mL/min. Each sample was centrifuged for 5 min at 3000 rpm, and the supernatant was used for injection. Semi-preparative HPLC was performed on either a HP 1100 Series system (Agilent Technologies) or an Alliance HPLC 2690 system (Waters), both equipped with a PDA detector. Data acquisition and processing were carried out with ChemStation software (Agilent Technologies) or Empower software (Waters), respectively. Semi-preparative separations were carried out on following on a SunFire Prep C_{18} column (5 μm, 150 × 10 mm i.d., Waters) equipped with a guard column (10 × 10 mm i.d.), a Xbridge Prep C_{18} (5 μm, 10 x 150 mm i.d., Waters), a ReproSil-Pur 120 C_{18}-AQ Prep column (3 μm, 150 × 10 mm i.d., Dr. Maisch GmbH) equipped with a guard column (10 × 10 mm i.d.), or a Nucleodur 100-5 CN column (5 μm, 150 × 10 mm i.d. Macherey-Nagel) equipped with a guard column (10 × 10 mm i.d.). All separations were carried out at a flow rate of 4 mL/min. Samples were centrifuged for 5 min at 3000 rpm prior to injection.

HPLC-PDA-ELSD-ESIMS analysis was performed on a LC-MS 8030 system (Shimadzu) consisting of degasser, binary high-pressure mixing pump, auto-sampler, column oven (CTO-20AC) and a PDA detector (SPD-M20A). An ELSD 3300 detector (Alltech) and a triple quadrupole MS were connected via a T-splitter to the system. A SunFire C18 column (3.5 μm, 150 × 3 mm i.d., Waters) equipped with a prep guard column (10 × 3 mm i.d.) was used at a flow rate of 0.4 mL/min. Mobile phases contained 0.1% formic acid (FA). HRESIMS spectra were recorded on a LTQ Orbitrap XL hybrid ion trap–orbitrap mass spectrometer (ThermoFisher Scientific).

TLC was carried out on Silica gel 60 F254 coated aluminium TLC plates (Merck). Detection was at 254nm and 366 nm, and by spraying with 1% vanillin in EtOH, followed by10% sulfuric acid in EtOH and heating at 110 °C for 10 min.

X-ray diffraction data for compound **2** were recorded on either a Bruker Kappa Apex 2 diffractometer, or a Stoe StadiVari diffractometer equipped with a Pilatus 300 K detector. The structure was solved with Superflip[45] and refined using Crystals.[46]

Plant Material. *Artemisia argyi* aerial parts were purchased from Peter Weinfurth, Bochum, Germany, in March 2016 (batch number 150788859). A voucher specimen (number 00 979) is deposited at the Division of Pharmaceutical Biology, University of Basel, Switzerland.

Extraction and Isolation. A large scale EtOAc extraction of *Artemisia argyi* and open column chromatography with the extract has been previously reported.[7] In short, a percolation of 400 g ground plant material with EtOAc (12 L) afforded 42 g of extract. Part of the extract (20g) was fractionated by column chromatography on silica gel with a gradient of n-hexane/EtOAc/MeOH [95:5:0 to 0:100:0 to 0:50:50] as mobile phase. Fractions I, J, L and N obtained from that first separation step were used in this work for further purification.

Fraction N (900 mg) was further separated by flash chromatography on a silica gel column (45 × 3.5 cm i.d.). The sample was introduced as dry load (900 mg adsorbed on 2.7 g silica gel), and elution performed with a gradient of MeOH (A) and $CHCl_3$ (B) [1% A (0-40 min), 1 → 10% A (40-120 min), 10 → 12.5% A (120-135 min), 12.5 → 20% A (135-155 min), 20 → 100% A (155-165 min), 100% A (165-200 min)]. Fractions were combined based on TLC ($CHCl_3$-MeOH, 95:5) patterns to fractions N_A to N_J. Fractions N_A, N_F, N_G and N_I were submitted to semi-preparative RP-HPLC on a Sunfire C_{18} column as follows (all solvents containing 0.1% FA): N_A (46.9 mg) with 38% CH_3CN, yielding **20** (1.5 mg, t_R 16.0) and **21** (1.8 mg, t_R 21.5). Fraction N_F (104.7 mg) with 30% CH_3CN, to afford **19** (35 mg, t_R 15.5) and

22 (3.9 mg, t_R 17.5). Fraction N_G (104.4 mg) and N_I (85.4mg) with 21% CH_3CN, yielding **2** (7.5 mg, t_R 18.9) and **10** (18 mg, t_R 17.2), respectively.

Fraction I (400 mg) was submitted to preparative RP-HPLC using a gradient of 40 → 100% CH_3CN + 0.1% FA (0–30 min), and 5 fractions (I_A to I_E) were obtained. Fraction I_B (50 mg) was submitted to semi-preparative RP-HPLC on a Sunfire C_{18} column using a gradient of 35 → 55% CH_3CN + 0.1% FA (0-30 min), followed by isocratic 55% CH_3CN + 0.1% FA (30-40 min). Fractions I_B_9 (5.6 mg) and I_B_10 (5.7 mg). These fractions were further purified by semi-prep RP-HPLC on a Xbridge C_{18} column with 53% CH_3CN, yielding compounds **4** (1.3 mg, t_R 38) and **3** (1.2 mg, t_R 41.0), respectively.

Fraction J (380 mg) was submitted to preparative RP-HPLC with 50% CH_3CN (0–30 min), to afford fractions J_A - J_D (J_A t_R 22.0, J_C t_R 25.0). Fractions J_A and J_C were submitted to semi-preparative RP-HPLC (all solvents containing 0.1% FA): J_A (30 mg) on a Nucleodur 100-5 CN column with 25% CH_3CN (0–30 min) to afford **8** (3 mg, t_R 37) and **7** (11.5 mg, t_R 39); J_C (30 mg) on a Xbridge C_{18} column with 37% CH_3CN, yielding **6** (2.5 mg, t_R 38.5) and **5** (9 mg, t_R 40.5).

Fraction O (500 mg) was submitted to preparative RP-HPLC with 32% CH_3CN, to afford fractions O_A - O_E (O_B t_R 10.6, O_D t_R 14.7, O_E t_R 24.0). Fraction O_B (18 mg) was submitted to semi-preparative RP-HPLC on a ReproSil-Pur 120 C_{18}-AQ column with 32% MeOH, yielding fraction O_B_6 (t_R 29.5) and **13a** (2.7 mg, t_R 34.0). O_B_6 (4 mg) was further purified by semi-preparative RP-HPLC on a Xbridge C_{18} column with 18% CH_3CN + 0.1% FA, to afford **12** (3.2 mg, t_R 17.5). Fractions O_D and O_E were submitted to semi-preparative RP-HPLC on a ReproSil-Pur 120 C_{18}-AQ column. Fraction O_D (28 mg) was separated with 32% MeOH to afford **14** (2.7 mg, t_R 21.0), and O_E (16 mg) with 52% MeOH to afford **18** (2.3 mg, t_R 15.5).

Fraction L (530 mg) was submitted to preparative RP-HPLC with a gradient of 30% → 100% CH_3CN (0–30 min) yielding in 9 fractions (L_A to L_I). Fraction L_A (30 mg) was submitted to semi-preparative RP-HPLC on a Xbridge C_{18} column with 19% CH_3CN, yielding two fractions (L_A_1 t_R 32.5, L_A_2 t_R 37.3). Fractions L_A_1 (5 mg) and L_A_2 (5 mg) were further purified by semi-preparative RP-HPLC on a Xbridge C_{18} column with 35% MeOH, to afford **15** (3.5 mg, t_R 17.5) and **16** (3 mg, t_R 18.5), respectively. Fraction L_B (55 mg) was separated by semi-preparative RP-HPLC on a Xbridge C_{18} column with 22% CH_3CN, to afford **11** (8 mg, t_R 29.5) and **9** (37 mg, t_R 36.5).

Fraction L_H (16 mg) was purified by semi-preparative RP-HPLC on a Xbridge C_{18} column with 70% MeOH + 0.1% FA, yielding **1** (1.5 mg, t_R 15.5).

Fraction L_I (9 mg) was submitted to semi-preparative RP-HPLC on a Xbridge C_{18} column with 65% CH_3CN, to afford **17** (5.2 mg, t_R 30.0).

All compounds were quality-controlled and showed a purity of over 90% based on HPLC-UV and NMR.

Artejasminolide (1): white solid; $[\alpha]_D^{25}$ +65 (*c* 1.22 mg/mL, $CHCl_3$); UV (MeOH) λ_{max} (log ε) 195 (4.3) nm; ECD (MeOH, *c* 0.71 mM, 0.1 cm); Δε +14.27 (199 nm), –6.9 (221 nm), +3.02 (304 nm); ^1H and ^{13}C NMR, see Table 1, Supporting Information; HRESIMS *m/z* 469.2572 $[M + H]^+$ (calcd for $C_{28}H_{37}O_6$, 469.2585).

8-Acetyl epiarteminolide (2): white solid; $[\alpha]_D^{25}$ -21 (*c* 0.9 mg/mL, MeOH); UV (MeOH) λ_{max} (log ε) 254 (3.9) nm; ECD (MeOH, *c* 0.61 mM, 0.1 cm); Δε +7.76 (195 nm), –4.41 (217 nm), +0.78 (246 nm), -1.78 (270 nm); ^1H and ^{13}C NMR, see Table 1, Supporting Information; HRESIMS *m/z* 549.2470 $[M + H]^+$ (calcd for $C_{32}H_{37}O_8$, 549.2483).

Argyinolide O (3): white solid; $[\alpha]_D^{25}$ +58 (*c* 1.03 mg/mL, MeOH); UV ($CHCl_3$) λ_{max} (log ε) 195 (4.2) nm; ECD (MeOH, *c* 0.48 mM, 0.1 cm); Δε +9.54 (210 nm), –1.63 (230 nm); ^1H and

^{13}C NMR, see Table 2, Supporting Information; HRESIMS *m/z* 347.1843 $[M + H]^+$ (calcd for $C_{20}H_{27}O_5$, 347.1853).

Argyinolide P (4): white solid; $[\alpha]_D^{25}$ +49 (*c* 1.12 mg/mL, MeOH); UV (MeOH) λ_{max} (log ε) 196 (4.3) nm; ECD (MeOH, *c* 0.48 mM, 0.1 cm); Δε +10.5 (208 nm), –1.52 (230 nm); ^{1}H and ^{13}C NMR, see Table 2, Supporting Information; ESIMS *m/z* 347 $[M+H]^+$.

Argyinolide Q (5): brown solid; $[\alpha]_D^{25}$ +59 (*c* 1 mg/mL, $CHCl_3$); UV (MeOH) λ_{max} (log ε) 253 (4.1) nm; ECD (MeOH, *c* 0.48 mM, 0.1 cm); Δε -1.47 (226 nm), +1.28 (246 nm), -2.21 (270 nm); ^{1}H and ^{13}C NMR, see Table 2, Supporting Information; HRESIMS *m/z* 345.1697 [M + H]$^+$ (calcd for $C_{20}H_{25}O_5$, 345.1697).

Artemdubolide C (6): brown solid; $[\alpha]_D^{25}$ +26 (*c* 0.78 mg/mL, $CHCl_3$); UV (MeOH) λ_{max} (log ε) 254 (4.0) nm; ECD (MeOH, *c* 0.48 mM, 0.1 cm); Δε -1.77 (226 nm), +0.77 (248 nm), -1.77 (271 nm); ^{1}H and ^{13}C NMR, see Table S1, Supporting Information; ESIMS *m/z* 345 $[M+H]^+$.

Moxartenolide (7): brown solid; $[\alpha]_D^{25}$ +72 (*c* 1.03 mg/mL, $CHCl_3$); UV (MeOH) λ_{max} (log ε) 253 (4.1) 254 (4.1) nm; ECD (MeOH, *c* 0.48 mM, 0.1 cm); Δε -1.16 (213 nm), +2.13 (246 nm), -1.99 (271 nm); ^{1}H and ^{13}C NMR, see Table S1, Supporting Information; ESIMS *m/z* 343 $[M+H]^+$.

Artemisiane E (8): white solid; $[\alpha]_D^{25}$ +55 (*c* 0.96 mg/mL, MeOH); UV (MeOH) λ_{max} (log ε) 213 (4.2) nm; ECD (MeOH, *c* 0.48 mM, 0.1 cm); Δε -2.34 (217 nm), +1.39 (246 nm), -2.55 (269 nm); ^{1}H and ^{13}C NMR, see Table S1, Supporting Information; ESIMS *m/z* 343 $[M+H]^+$

11,13-Dehydromatricarin (9): brown solid; $[\alpha]_D^{25}$ +73 (*c* 1.04 mg/mL, MeOH); UV ($CHCl_3$) λ_{max} (log ε) 254 (4.1) nm; ECD (MeOH, *c* 0.55 mM, 0.1 cm); Δε -1.63 (221 nm), +1.6 (246 nm), -2.66 (269 nm); ^{1}H and ^{13}C NMR, see Table S2, Supporting Information; ESIMS *m/z* 303 $[M+H]^+$.

11,13-Dehydrodesacetylmatricarin (10): white solid; $[\alpha]_D^{25}$ +54 (*c* 0.85 mg/mL, MeOH); UV (MeOH) λ_{max} (log ε) 254 (4.1) nm; ECD (MeOH, *c* 0.64 mM, 0.1 cm); Δε +17.34 (195

nm), -1.45 (226 nm), +1.99 (246 nm), -2.46 (275 nm); ^{1}H and ^{13}C NMR, see Table S2, Supporting Information; ESIMS *m/z* 261 $[M+H]^+$.

Dehydroleucodine (11): brown solid; $[\alpha]_D^{25}$ +58 (*c* 0.93 mg/mL, MeOH); UV (MeOH) λ_{max} (log ε) 195 (4.2) 254 (4.1) nm; ECD (MeOH, *c* 0.34 mM, 0.1 cm); Δε +10.23 (195 nm), -2.1 (217 nm), +3.58 (251 nm), -0.93 (276 nm); ^{1}H and ^{13}C NMR, see Table S2, Supporting Information; ESIMS *m/z* 245 $[M+H]^+$.

Artecalin (12): white solid; $[\alpha]_D^{25}$ +29 (*c* 1.08 mg/mL, MeOH); UV (MeOH) λ_{max} (log ε) 203 (4.0) nm; ECD (MeOH, *c* 1.26 mM, 0.1 cm); Δε +8.56 (200 nm), -0.85 (253 nm), +0.88 (289 nm); ^{1}H and ^{13}C NMR, see Table S3, Supporting Information; ESIMS *m/z* 265 $[M+H]^+$.

Armexifolin (13a): white solid; $[\alpha]_D^{25}$ +64 (*c* 1.05 mg/mL, $CHCl_3$); UV (MeOH) λ_{max} (log ε) 202 (4.0) 240 (4.0) nm; ECD (MeOH, *c* 1.27 mM, 0.1 cm); Δε +5.1 (200 nm), +9.7 (245 nm), -1.11 (323 nm); ^{1}H and ^{13}C NMR, see Table S3, Supporting Information; ESIMS *m/z* 263 $[M+H]^+$.

Methyl 2-[(1S,2S,4aR,5R)-1,5-dihydroxy-4a,8-dimethyl-7-oxo-1,2,3,4,4a,5,6,7-octahydronaphthalen-2-yl]prop-2-enoate (13b): white solid; UV (MeOH) λ_{max} (log ε) 252 (3.8) nm; ECD (MeOH, *c* 1.13 mM, 0.1 cm); Δε -0.59 (207 nm), +5.02 (252 nm), -0.89 (309 nm); ^{1}H and ^{13}C NMR, see Table S3, Supporting Information; HRESIMS *m/z* 295.1543 $[M + H]^+$ (calcd for $C_{16}H_{23}O_{55}$, 295.1540).

3-O-Acetyl-iso-seco-tanapartholide (14): brown solid; $[\alpha]_D^{25}$ -3 (*c* 1.18 mg/mL, MeOH); UV (MeOH) λ_{max} (log ε) 221 (4.3) nm; ECD (MeOH, *c* 0.51 mM, 0.1 cm); Δε -7.22 (195 nm), +23.73 (223 nm), -4.1 (321 nm); ^{1}H and ^{13}C NMR, see Table S3, Supporting Information; ESIMS *m/z* 321 $[M+H]^+$.

Arteglasin B (15): white solid; $[\alpha]_D^{25}$ +134 (*c* 1.18 mg/mL, MeOH); UV (MeOH) λ_{max} (log ε) 195 (4.2) nm; ECD (MeOH, *c* 0.52 mM, 0.1 cm); Δε +12.78 (197 nm), -1.39 (228 nm); ^{1}H and ^{13}C NMR, see Table S4, Supporting Information; ESIMS *m/z* 321 $[M+H]^+$.

Argyinolide R (16): white solid; $[\alpha]_D^{25}$ +108 (*c* 1.02 mg/mL, MeOH); UV (MeOH) λ_{max} (log ε) 195 (4.2) nm; ECD (MeOH, *c* 0.52 mM, 0.1 cm); Δε +3.28 (208 nm), -0.71 (257 nm); ^{1}H and ^{13}C NMR, see Table S4, Supporting Information; ESIMS *m/z* 343 $[M+Na]^+$.

Artemisolide (17): white solid; $[\alpha]_D^{25}$ -52 (*c* 1.21 mg/mL, MeOH); UV (MeOH) λ_{max} (log ε) 204 (4.1) nm; ECD (MeOH, *c* 0.84 mM, 0.1 cm); Δε +10.81 (195 nm), -12.68 (224 nm), -0.75 (311 nm); ^{1}H and ^{13}C NMR, see Table S5, Supporting Information; ESIMS *m/z* 397 $[M+H]^+$.

(-)Jasmonic acid (18): brown solid; $[\alpha]_D^{25}$ -58 (*c* 0.98 mg/mL, MeOH); UV (MeOH) λ_{max} (log ε) 195 (3.8) nm; ECD (MeOH, *c* 0.78 mM, 0.1 cm); Δε -2.14 (299 nm);^{1}H and ^{13}C NMR, see Table S5, Supporting Information; ESIMS *m/z* 211 $[M+H]^+$.

Jaceosidin (19): yellow solid; ^{1}H and ^{13}C NMR were recently reported[6]; ESIMS *m/z* 331 $[M+H]^+$.

Eupatilin (20): yellow solid; ^{1}H and ^{13}C NMR were recently reported[6]; ESIMS *m/z* 345 $[M+H]^+$.

Chrysosplenitin (21): yellow solid; ^{1}H and ^{13}C NMR were recently reported[6]; ESIMS *m/z* 375 $[M-H]^-$.

6-Methoxytricin (22): yellow solid; ^{1}H and ^{13}C NMR were, recently reported[6]; ESIMS *m/z* 361 $[M+H]^+$.

Cell Lines and Cell Culture. Details on cell line construction and culture conditions have been reported.[4] In brief, MM121224 and A2058 cells were transfected to stably express H2B-mTurquoise, ERK-KTR-mScarlet, and FoxO3a-KTR-mNeonGreen.

Immunostaining. Immunostaining was done as previously described.[4] In brief, MM121224 wild-type cells were treated with primary antibodies (Monoclonal Anti-MAP Kinase, Activated (diphosphorylated ERK-1&2), Sigma-Aldrich; Phospho-Akt (Ser473), Cell Signaling Technology) and secondary antibodies (Alexa 546 goat anti-mouse and Alexa 546 goat anti-mouse; both Life Technolgies/Thermofisher).

High-content assay. The high-content assay was performed as previously described.[4] In brief, the cell lines were seeded in 96-well plates and incubated with extracts (75 μg/mL), fractions (75 μg/mL), or pure compounds (200 μM to 1.56 μM). After fixation, images were acquired with a HCS microscope. Image processing and analysis was done with Cellprofiler 2.3.1 software and custom scripts written in R programming language.

Computational methods. Conformational analysis was performed with MacroModel (Schrödinger Release 2020-2, LLC, New York) employing the OPLS2005 (optimized potential for liquid simulations) force field in H_2O for geometrical optimization in two steps. In the first step, a global minimum was searched using 30,000 steps, in the second step, the global minimum was the iput to a conformational search over 10,000 steps and the ten conformers with the lowest energies were the input to ab initio calculations. First, the geometry was optimized and the energy calculated by applying DFT at the CAM-B3LYP/Def2SVP level of theory, and employing the SCRF method and the CPMC model for solvation in MeOH with the Gaussian 09 program package.[47] Excitation energy (denoted by wavelength in nm), rotator strength (R_{str}), dipole velocity (R_{vel}), and dipole length (R_{len}) were calculated in MeOH by TD-DFT at the same level of theory. The plotted ECD curves were then obtained on the basis of rotator strengths with a half-band of 0.25 eV and a shift of the spectra by +10 nm using SpecDis v1.71.[48]

Conformational analysis for compounds 15 and 16. Both compounds were subjected to conformational searches using the OPLS3e force field in the gas phase alone (for i) as well as including one water molecule (for ii and iii), which was randomly placed in the vicinity of the studied molecule and assigned as the movable fragment in MacroModel (Schrödinger Release 2020-2, LLC, New York). For each molecular system 1000 search steps were performed using mixed torsional low-mode sampling method. Conformers within the energy window of 5.0

kcal/mol were saved for further processing (number of conformers: **15**: 11; **15**+H_2O: 20; **16**: 7; **16**+H_2O: 20) as decribed before.

ASSOCIATED CONTENT

Supporting Information.

Additional details on the targeted pathways, additional HPLC-based activity profiles, NMR spectra for all known compounds, calculated and experimental ECD and UV spectra for all compounds, table of crystallographic data, additional LC-MS traces (for **13b**), an overview of the different sesquiterpene lactone dimers, concentration-response curves for all compounds on AKT signaling, and microscopic images to demonstrate activity for selected compounds.

AUTHOR INFORMATION

Notes

The authors declare no competing financial interest.

ACKNOWLEDGMENTS

Thanks are due to Alberto Mattei for providing the transfected A2058 and MM121224 cell lines (Division of Cell Biology, University of Bern), Mitchell Levesque (University Hospital of Zurich) for providing the MM121224 cell line, and Matthias Wymann (Department of Biomedicine, University of Basel) for the A2058 cell line. We acknowledge the DBM Microscopy Core Facility (Department of Biomedicine, University of Basel) for providing access to their HCS microscope, and Pascal Lorentz for technical support in microscopy. We are grateful to Vanessa Abegg for recording of HRESIMS spectra (Division of Pharmaceutical Biology, University of Basel), and to Dr. Alessandro Prescimone at the Laboratory Chemical Crystallography for X-ray diffraction analysis (University of Basel). We want to thank Anika

John for her work on the random forest model. We acknowledge the Swiss National Science Foundation for their financial support (Project no 205321-176008).

REFERENCES

(1) Matthews, N. H.; Li, W.-Q.; Qureshi, A. A.; Weinstock, M. A.; Cho, E. In *Cutaneous Melanoma: Etiology and Therapy*; Ward, W. H., Farma, J. M., Eds.; Codon Publications: Brisbane (AU), 2017.

(2) Yajima, I.; Kumasaka, M. Y.; Thang, N. D.; Goto, Y.; Takeda, K.; Yamanoshita, O.; Iida, M.; Ohgami, N.; Tamura, H.; Kawamoto, Y.; Kato, M. *Dermatol. Res. Pract.* **2012**, *2012*, 354191.

(3) Tanda, E. T.; Vanni, I.; Boutros, A.; Andreotti, V.; Bruno, W.; Ghiorzo, P.; Spagnolo, F. *Front. Mol. Biosci.* **2020**, *7*, 154.

(4) Dürr, L.; Hell, T.; Dobrzyński, M.; Mattei, A.; John, A.; Augsburger, N.; Bradanini, G.; Reinhardt, J. K.; Rossberg, F.; Drobnjakovic, M.; Gupta, M. P.; Hamburger, M.; Pertz, O.; Garo, E. *J. Nat. Prod.* **2022**, *85*, 1006–1017.

(5) Potterat, O.; Hamburger, M. *Planta Med.* **2014**, *80*, 1171–1181.

(6) Hell, T.; Rutz, A.; Dürr, L.; Dobrzyski, M.; Reinhardt, J. K.; Lehner, T.; Keller, M.; John, A.; Gupta, M. P.; Pertz, O.; Hamburger, M.; Wolfender, J.-L.; Garo, E. *J. Nat. Prod.* **2022**. Manuscript accepted for publication.

(7) Reinhardt, J. K.; Klemd, A. M.; Danton, O.; De Mieri, M.; Smieško, M.; Huber, R.; Bürgi, T.; Gründemann, C.; Hamburger, M. *J. Nat. Prod.* **2019**, *82*, 1424–1433.

(8) Xi, X.; Liu, N.; Wang, Q.; Chu, Y.; Yin, Z.; Ding, Y.; Lu, Y. *Cell Death Dis.* **2019**, *10*, 1–17.

(9) Tong, L.; Li, J.; Li, Q.; Wang, X.; Medikonda, R.; Zhao, T.; Li, T.; Ma, H.; Yi, L.; Liu, P.; Xie, Y.; Choi, J.; Yu, S.; Lin, Y.; Dong, J.; Huang, Q.; Jin, X.; Lim, M.; Yang, X. *Theranostics* **2020**, *10*, 5943–5956.

(10) Kim, J. G.; Lee, J. W.; Le, T. P. L.; Han, J. S.; Cho, Y. B.; Kwon, H.; Lee, D.; Lee, M. K.; Hwang, B. Y. *J. Nat. Prod.* **2021**, *84*, 562–569.

(11) Huang, Z.-S.; Pei, Y.-H.; Liu, C.-M.; Lin, S.; Tang, J.; Huang, D.-S.; Song, T.-F.; Lu, L.-H.; Gao, Y.-P.; Zhang, W.-D. *Planta Med.* **2010**, *76*, 1710–1716.

(12) Okunade, A. L.; Liu, S.; Clark, A. M.; Hufford, C. D.; Rogers, R. D. *Phytochemistry* **1993**, *35*, 191–194.

(13) Xue, G.-M.; Xue, J.-F.; Zhao, C.-G.; Zhao, Z.-Z.; Sun, Y.-J.; Du, K.; Li, H.-W.; Feng, W.-S. *Nat. Prod. Res.* **2021**, *35*, 2887–2894.

(14) Bohlmann, F.; Zdero, C. *Phytochemistry* **1978**, *17*, 1595–1599.

(15) Lee, S.-H.; Kang, H.-M.; Song, H.-C.; Lee, H.; Lee, U. C.; Son, K.-H.; Kim, S.-H.; Kwon, B.-M. *Tetrahedron* **2000**, *56*, 4711–4715.

(16) Ohno, N.; Gershenzon, J.; Roane, C.; Mabry, T. J. *Phytochemistry* **1980**, *19*, 103–106.

(17) Bohlmann, F.; Zdero, C. *Tetrahedron Lett.* **1972**, *13*, 621–624.

(18) Ordóñez, P. E.; Quave, C. L.; Reynolds, W. F.; Varughese, K. I.; Berry, B.; Breen, P. J.; Malagón, O.; Smeltzer, M. S.; Compadre, C. M. *J. Ethnopharmacol.* **2011**, *137*, 1055–1059.

(19) Geissman, T. A.; Griffin, T. S.; Irwin, M. A. *Phytochemistry* **1969**, *8*, 1297–1300.

(20) Ahmed, A. A.; Gáti, T.; Hussein, T. A.; Ali, A. T.; Tzakou, O. A.; Couladis, M. A.; Mabry, T. J.; Tóth, G. *Tetrahedron* **2003**, *59*, 3729–3735.

(21) Mata, R.; Delgado, G.; de Vivar, A. R. *Phytochemistry* **1984**, *23*, 1665–1668.

(22) Moiseeva, G. P.; Yusupova, I. M.; Kasymov, Sh. Z.; Yusupov, M. I. *Chem. Nat. Compd.* **1982**, *18*, 295–297.

(23) Tan, R. X.; Jia, Z. J.; Jakupovic, J.; Bohlmann, F.; Huneck, S. *Phytochemistry* **1991**, *30*, 3033–3035.

(24) Lee, K. H.; Matsueda, S.; Geissman, T. A. *Phytochemistry* **1971**, *10*, 405–410.

(25) Ahmed, A. A.; Mahmoud, A. A.; Hegazy, M. F.; Paré, P. W.; Karchesy, J. *Pharm.* **2002**, *57*, 567–569.

(26) Kim, J. H.; Kim, H.-K.; Jeon, S. B.; Son, K.-H.; Kim, E. H.; Kang, S. K.; Sung, N.-D.; Kwon, B.-M. *Tetrahedron Lett.* **2002**, *43*, 6205–6208.

(27) Husain, A.; Ahmad, A.; Agrawal, P. K. *J. Nat. Prod.* **1993**, *56*, 2008–2011.

(28) Martínez, V.; Barberá, O.; Sánchez-Parareda, J.; Alberto Marco, J. *Phytochemistry* **1987**, *26*, 2619–2624.

(29) Lan, J.-E.; Li, X.-J.; Zhu, X.-F.; Sun, Z.-L.; He, J.-M.; Zloh, M.; Gibbons, S.; Mu, Q. *Nat. Prod. Res.* **2021**, *35*, 1881–1886.

(30) Liu, Y.; Mabry, T. J. *Phytochemistry* **1981**, *20*, 309–311.

(31) Ma, L.-F.; Chen, Y.-L.; Shan, W.-G.; Zhan, Z.-J. *Nat. Prod. Rep.* **2020**, *37*, 999–1030.

(32) Lee, S.-H.; Kim, H.-K.; Seo, J.-M.; Kang, H.-M.; Kim, J. H.; Son, K.-H.; Lee, H.; Kwon, B.-M.; Shin, J.; Seo, Y. *J. Org. Chem.* **2002**, *67*, 7670–7675.

(33) Lee, S.-H.; Kim, M.-J.; Bok, S. H.; Lee, H.; Kwon, B.-M.; Shin, J.; Seo, Y. *J. Org. Chem.* **1998**, *63*, 7111–7113.

(34) Jakupovic, J.; Chen, Z.-L.; Bohlmann, F. *Phytochemistry* **1987**, *26*, 2777–2779.

(35) Creelman, R. A.; Mullet, J. E. *Annu. Rev. Plant Physiol. Plant Mol. Biol.* **1997**, *48*, 355–381.

(36) Mueller, M. J. *Physiol. Plant.* **1997**, *100*, 653–663.

(37) Schmidt, T. J. Atta-ur-Rahman, Ed.; Elsevier, 2006; Vol. 33, pp 309–392.

(38) Kupchan, S. M.; Eakin, M. A.; Thomas, A. M. *J. Med. Chem.* **1971**, *14*, 1147–1152.

(39) Fernandes, M. B.; Scotti, M. T.; Ferreira, M. J. P.; Emerenciano, V. P. *Eur. J. Med. Chem.* **2008**, *43*, 2197–2205.

(40) Kupchan, S. M.; Fessler, D. C.; Eakin, M. A.; Giacobbe, T. J. *Science* **1970**, *168*, 376–378.

(41) Schmidt, T. J. *Bioorg. Med. Chem.* **1997**, *5*, 645–653.

(42) Lickliter, J. D.; Jennens, R.; Lemech, C. R.; Kichenadasse, G.; Cai, D.; Su, S. Y.-C. *J. Clin. Oncol.* **2021**, *39*, 2037–2037.

(43) Molina, D. M.; Jafari, R.; Ignatushchenko, M.; Seki, T.; Larsson, E. A.; Dan, C.; Sreekumar, L.; Cao, Y.; Nordlund, P. *Science* **2013**, *341*, 84–87.

(44) Franken, H.; Mathieson, T.; Childs, D.; Sweetman, G. M. A.; Werner, T.; Tögel, I.; Doce, C.; Gade, S.; Bantscheff, M.; Drewes, G.; Reinhard, F. B. M.; Huber, W.; Savitski, M. M. *Nat. Protoc.* **2015**, *10*, 1567–1593.

(45) Palatinus, L.; Chapuis, G. *J. Appl. Crystallogr.* **2007**, *40*, 786–790.

(46) Betteridge, P. W.; Carruthers, J. R.; Cooper, R. I.; Prout, K.; Watkin, D. J. *J. Appl. Crystallogr.* **2003**, *36*, 1487–1487.

(47) Frisch, M. J.; Trucks, G. W.; Schlegel, H. B.; Scuseria, G. E.; Robb, M. A.; Cheeseman, J. R.; Scalmani, G.; Barone, V.; Petersson, G. A.; Nakatsuji, H.; Li, X.; Caricato, M.; Marenich, A.; Bloino, J.; Janesko, B. G.; Gomperts, R.; Mennucci, B.; Hratchian, H. P.; Ortiz, J. V.; Izmaylov, A. F.; Sonnenberg, J. L.; Williams-Young, D.; Ding, F.; Lipparini, F.; Egidi, F.; Goings, J.; Peng, B.; Petrone, A.; Henderson, T.; Ranasinghe, D.; Zakrzewski, V. G.; Gao, J.; Rega, N.; Zheng, G.; Liang, W.; Hada, M.; Ehara, M.; Toyota, K.; Fukuda, R.; Hasegawa, J.; Ishida, M.; Nakajima, T.; Honda, Y.; Kitao, O.; Naka, H.; Vreven, T.; Throssell, K.; Montgomery, J. A.; Peralta, J. E.; Ogliaro, F.; Bearpark, M.; Heyd, J. J.; Brothers, E.; Kudin, K. N.; Staroverov, V. N.; Keith, T.; Kobayashi, R.; Normand, J.; Raghavachari, K.; Rendel, A.; Burant, J. C.; Iyengar, S. S.; Tomasi, J.; Cossi, M.; Millam, J. M.; Klene, M.; Adamo, C.; Cammi, R.; Ochterski, J. W.; Martin, R. L.; Morokuma, K.; Farkas, O.; Foresman, J. B.; Fox, D. J. *Gaussian 09, Revision D.01*.

(48) Bruhn, T.; Schaumlöffel, A.; Hemberger, Y.; Bringmann, G. *Chirality* **2013**, *25*, 243–249.

Graphical Abstract